Proceedings of the
47th IEEE Conference on Decision and Control
Cancun, Mexico, Dec. 9-11, 2008

Tracking analysis of an adaptive vibration controller

Maciej Niedźwiecki and Michał Meller
Faculty of Electronics, Telecommunications and Computer Science
Department of Automatic Control, Gdańsk University of Technology
ul. Narutowicza 11/12, Gdańsk, Poland
maciekn@eti.pg.gda.pl , michal.meller@eti.pg.gda.pl

Abstract— **The problem of rejection of a sinusoidal disturbance of known frequency, acting at the output of a discrete-time complex-valued linear stable plant with unknown dynamics, is considered. It is assumed that output signal is contaminated with wideband measurement noise. The paper presents convergence and tracking analysis of a new narrow-band disturbance elimination scheme described recently. It is shown that the proposed adaptive feedback regulator converges locally in the mean to the optimal (minimum-variance) regulator. It is also shown that it has very good robustness properties.**

Index Terms: Adaptive control, system identification, disturbance rejection.

I. INTRODUCTION

Consider the problem of reduction of a narrow-band disturbance at the output of a discrete-time complex-valued system governed by

$$y(t) = K_o(q^{-1})u(t-1) + d(t) + v(t) \tag{1}$$

where $t = \ldots, -1, 0, 1, \ldots$ denotes normalized time, q^{-1} is the backward shift operator, $y(t)$ denotes the corrupted complex-valued system output, $K_o(q^{-1})$ denotes unknown transfer function of a linear single-input single-output stable plant, $d(t)$ given by

$$d(t) = a(t)e^{j\omega_o t} \tag{2}$$

is a complex-valued sinusoidal disturbance (cisoid) of known frequency ω_o and unknown, slowly varying amplitude $a(t)$, $v(t)$ is a wideband measurement noise and, finally, $u(t)$ denotes the input (controlled) signal.

In this study we will assume that no reference signal is available, i.e. one has access to the output signal only. We will look for a feedback controller allowing for cancellation, or near-cancellation, of the sinusoidal disturbance, i.e. controller generating the complex-valued feedback signal $u(t)$ that minimizes system output in the mean-squared sense: $\mathrm{E}[\,|\,y(t)\,|^2\,] \longmapsto \min$.

The need for vibration control arises in many electro-mechanical systems, where narrow-band disturbances are usually generated by rotating machinery and their suppression is necessary to maintain high quality of the underlying technological process [1]. Similar problems are encountered in active noise control systems, where the unwanted sound is attenuated by a noise-canceling speaker emitting a sound wave with the same amplitude but opposite polarity [2]. Both types of applications fall into a more general narrow-band disturbance rejection category.

The problem of narrow-band disturbance rejection was considered by many authors under different methodologies (internal model principle, phase-locked loop approach) – see e.g. the recent work of Bodson and co-workers [3], [4], and Landau and co-workers [5], [6]; a good overview of different approaches can be found e.g. in a tutorial paper [6].

An entirely new approach to cancellation of narrow-band disturbances, based on coefficient fixing and automatic gain tuning, was recently proposed and analyzed in [7]. Suppose that the measurement noise in (1) obeys

(**A1**) $\{v(t)\}$ is a zero-mean circular white sequence with variance σ_v^2.

and that the coefficient $a(t)$ in (2) evolves according to the random-walk (RW) model

$$a(t) = a(t-1) + w(t) \tag{3}$$

where the sequence of one-step changes obeys

(**A2**) $\{w(t)\}$, independent of $\{v(t)\}$, is a zero-mean circular white sequence with variance σ_w^2.

Additionally, suppose that the unknown plant is stable and has nonzero gain at the frequency ω_o:

(**A3**) $K_o(q^{-1}) = \sum_{i=0}^{\infty} f_i q^{-i},\ \ \sum_{i=0}^{\infty} |\,f_i| < \infty,$
$K_o(e^{-j\omega_o}) \neq 0$.

Under (A1)–(A3) the minimum variance control rule, i.e. the rule that minimizes the steady-state mean-squared output error $\mathrm{E}_\infty[|y(t)|^2] = \lim_{t\mapsto\infty} \mathrm{E}[|y(t)|^2]$ has the form [7]

$$\widehat{d}(t+1|t) = e^{j\omega_o}[\,\widehat{d}(t|t-1) + \mu_o y(t)\,]$$
$$u(t) = -\frac{\widehat{d}(t+1|t)}{k_o} \tag{4}$$

where μ_o is the real-valued adaptation gain given in the form

$$\mu_o = -\,\xi/2 + \sqrt{\xi^2/4 + \xi}\ , \quad \xi = \sigma_w^2/\sigma_v^2 \tag{5}$$

and $k_o = K_o(e^{-j\omega_o})$ is the true plant gain.

The derivation of (4) was based on the following steady-state approximation

$$K_o(q^{-1})u(t-1) \cong k_o u(t-1) \tag{6}$$

which holds for a narrow-band signal $u(t)$.[1]

[1] Vaguely speaking, to cancel sinusoidal disturbance $d(t)$, one should generate such sinusoidal signal $u(t)$ that after passing through the plant will have the same amplitude as $d(t)$, but opposite polarity. Hence, the narrow-band assumption made on $u(t)$ is certainly justified.

When the plant's gain is unknown, one can replace it with the "nominal" gain $k_n = K_n(e^{-j\omega_o}) \neq 0$, where $K_n(q^{-1})$ denotes nominal (assumed) transfer function. This results in the algorithm

$$\begin{aligned} \widehat{d}(t+1|t) &= e^{j\omega_o}[\, \widehat{d}(t|t-1) + \mu y(t)\,] \\ u(t) &= -\frac{\widehat{d}(t+1|t)}{k_n} \quad . \end{aligned} \tag{7}$$

Interestingly, even though in general the assumed plant's gain differs from the true one, i.e. $\beta = k_o/k_n \neq 1$, when the adaptation gain satisfies

$$\mu\beta = \mu_o \tag{8}$$

the mean-squared output error yielded by (7) is identical with that observed for the optimal algorithm (4). This means that, for a proper choice of μ, the modeling bias is automatically compensated by feedback.

Note that, according to (8), in the presence of phase modeling errors ($\mathrm{Im}\beta \neq 0$), the optimal adaptation gain $\mu = \mu_o/\beta$ is complex-valued. The gain μ can be optimized on-line using the recursive prediction error (RPE) approach. The resulting self-tuning disturbance rejection regulator can be summarized as follows

$$\begin{aligned} z(t) = e^{j\omega_o}[\, & (1 - |\,\widehat{\mu}(t-1)|\,)z(t-1) \\ & - \frac{|\,\widehat{\mu}(t-1)|}{\widehat{\mu}(t-1)}\, y(t-1)\,] \end{aligned} \tag{9}$$

$$\begin{aligned} r(t) &= \rho r(t-1) + |\,z(t)|^2 \\ \widehat{\mu}(t) &= \widehat{\mu}(t-1) - \frac{z^*(t)y(t)}{r(t)} \\ \widehat{d}(t+1|\,t) &= e^{j\omega_o}[\, \widehat{d}(t|\,t-1) + \widehat{\mu}(t)y(t)\,] \\ u(t) &= -\frac{\widehat{d}(t+1|\,t)}{k_n} \end{aligned} \tag{10}$$

where $z(t)$ is the local estimate of the sensitivity derivative $\partial y(t;\mu)/\partial\mu$, $*$ denotes complex conjugation and ρ, $(0 < \rho < 1)$ is the user-dependent forgetting constant that determines the effective width of the local analysis interval, equal to $1/(1-\rho)$ samples – see [7] for more details.

For practical reasons that will be explained later, (9) can be replaced with

$$z(t) = e^{j\omega_o}[\, (1 - c_\mu)z(t-1) - \frac{c_\mu}{\widehat{\mu}(t-1)}\, y(t-1)\,] \tag{11}$$

where c_μ is a small positive constant.

Both the original algorithm (9)–(10), and its modified version (10)–(11), were tested in [7] in several simulation experiments, showing satisfactory convergence and robustness properties. The main purpose of the current submission is to provide theoretical explanation of this experimentally observed behavior. We will show that, under assumptions (A1)–(A3), the proposed regulator converges (locally) in the mean to the optimal regulator, i.e. that

$$\mathrm{E}_\infty[\widehat{\mu}(t)] \cong \frac{\mu_o}{\beta} \quad . \tag{12}$$

Our analysis will also shed light on the role played by design variables ρ and c_μ.

Of course, most of the signals and systems encountered in practice are real-valued. Even though the algorithms studied in this paper are not ready-for-use solutions applicable to the real case – such solutions are presented in a companion paper [8] – all qualitative conclusions of the analysis carried out below remain valid for real-valued algorithms.

II. Tracking analysis

In this section we will study tracking properties of the algorithm (10)–(11). Our analysis will be based on examining properties of a stochastic differential equation (SDE) associated with the disturbance rejection algorithm. Since strict mathematical conditions, under which such SDE-based approach is applicable, are not specified (one of the prerequisites is stochastic stability of the analyzed system, which is a difficult problem to resolve on its own), the "theoretical" results derived below must be carefully experimentally verified. This will be done in Section IV.

To avoid unnecessary complications, we will examine tracking properties of the simplified (gradient) version of the algorithm (10)–(11), given in the form

$$\widehat{\mu}(t) = \widehat{\mu}(t-1) - \alpha y(t)z^*(t) \tag{13}$$

where $\alpha > 0$ denotes a small gain. Later on we will extend results of our analysis to the normalized case, where the constant gain is replaced with recursively computed normalizing factor $1/r(t)$.

It is known that tracking behavior of constant-gain (finite-memory) estimation algorithms, such as (13), can be studied by examining properties of the associated difference equations. Denote by $\{y(t;\mu)\}$ and $\{z(t;\mu)\}$ stationary processes that "settle down" in the closed-loop system for a constant value of μ: $\widehat{\mu}(t) \equiv \mu \in \Omega_s$, where Ω_s is the stability region. Furthermore, let $\mu_\star$ be the stable "equilibrium" point of (13) obeying

$$f(\mu_\star) = 0 \tag{14}$$

$$\mathrm{Re}[f'(\mu_\star)] > 0 \tag{15}$$

where

$$f(\mu) = \mathrm{E}[y(t;\mu)z^*(t;\mu)]$$

and $f'(\mu) = \partial f(\mu)/\partial\mu$. The (symbolic) differentiation with respect to a complex variable is defined as [11]

$$\frac{\partial}{\partial\mu} = \frac{1}{2}\left[\frac{\partial}{\partial\mathrm{Re}[\mu]} - j\,\frac{\partial}{\partial\mathrm{Im}[\mu]}\right] \quad .$$

According to [9], [10], when the coefficient α is sufficiently small the evolution of the estimation error $\widehat{\mu}(t) - \mu_\star$ can be approximately described by the following linearized stochastic differential equation (provided that tracking is satisfactory, i.e. $\widehat{\mu}(t)$ remains close to $\mu_\star$)

$$\begin{aligned} dX_s &= -\alpha f'(\mu_\star)X_s ds + \alpha\sqrt{g(\mu_\star)}\, dW_s \\ X_s &\cong \widehat{\mu}(t) - \mu_\star \quad \text{for} \quad s = t \end{aligned} \tag{16}$$

where

$$g(\mu) = \sum_{\tau=-\infty}^{\infty} \mathrm{E}\,[\, y(\tau;\mu)z^*(\tau;\mu)y^*(0;\mu)z(0;\mu)\,] \tag{17}$$

(the series being assumed convergent) and $\{W_s\}$ denotes a standard complex-valued Wiener process.

A. Equilibrium point

We will show that the equilibrium point of (13) obeys (8), i.e. $\mu_\star = \mu_o/\beta$. For two jointly stationary processes $\{x(t)\}$ and $\{y(t)\}$ define $R_{xy}(\tau) = \mathrm{E}[x(t)y^*(t-\tau)]$. Note that $f(\mu) = R_{yz}(0;\mu)$. Using the steady-state approximation (6) one arrives at

$$\begin{aligned} y(t) = (1-\mu\beta)e^{j\omega_o}y(t-1) + e^{j\omega_o t}w(t) \\ + v(t) - e^{j\omega_o}v(t-1) \end{aligned} \tag{18}$$

(for the sake of brevity the dependence on μ is temporarily dropped). Combining (11) with (18) one obtains

$$\begin{aligned} \mathrm{E}[y(t)z^*(t)] = \mathrm{E}\big\{\big[(1-\mu\beta)e^{j\omega_o}y(t-1) \\ + e^{j\omega_o t}w(t) + v(t) - e^{j\omega_o}v(t-1)\big] \\ \times \big[(1-c_\mu)e^{-j\omega_o}z^*(t-1) - \frac{c_\mu}{\mu^*}\ e^{-j\omega_o}y^*(t-1)\big]\big\} \end{aligned}$$

which, after elimination of cross terms that are zero due to orthogonality, leads to the following recursive relationship

$$\begin{aligned} R_{yz}(0) = (1-c_\mu)(1-\mu\beta)R_{yz}(0) \\ - \frac{c_\mu}{\mu^*}(1-\mu\beta)R_{yy}(0) + \frac{c_\mu}{\mu^*}R_{vy}(0)\ . \end{aligned} \tag{19}$$

In an analogous way the relationship

$$\begin{aligned} \mathrm{E}[y(t)y^*(t)] = \mathrm{E}\big\{\big[(1-\mu\beta)e^{j\omega_o}y(t-1) \\ + e^{j\omega_o t}w(t) + v(t) - e^{j\omega_o}v(t-1)\big] \\ \times \big[(1-\mu^*\beta^*)e^{-j\omega_o}y^*(t-1) + e^{-j\omega_o t}w^*(t) \\ + v^*(t) - e^{-j\omega_o}v^*(t-1)\big]\big\} \end{aligned}$$

implies

$$\begin{aligned} R_{yy}(0) = |1-\mu\beta|^2 R_{yy}(0) + \sigma_w^2 + 2\sigma_v^2 \\ - (1-\mu\beta)R_{yv}(0) - (1-\mu^*\beta^*)R_{vy}(0)\ . \end{aligned} \tag{20}$$

Note that $R_{yv}(0) = R_{vy}(0) = \sigma_v^2$. Solving (19) and (20) with respect to $R_{yy}(0)$ and $R_{yz}(0)$ one obtains

$$R_{yy}(0) = \frac{\sigma_w^2 + |\mu\beta|^2\sigma_v^2}{1-|1-\mu\beta|^2} + \sigma_v^2 \tag{21}$$

$$R_{yz}(0) = -\frac{c_\mu[(1-\mu\beta)R_{yy}(0) - \sigma_v^2]}{[1-(1-c_\mu)(1-\mu\beta)]\mu^*}\ . \tag{22}$$

The equilibrium point $\mu_\star$ can be determined by solving $f(\mu_\star) = R_{yz}(0;\mu_\star) = 0$ or equivalently

$$(1-\mu_\star\beta)R_{yy}(0;\mu_\star) = \sigma_v^2\ . \tag{23}$$

Let $x_\star = 1 - \mu_\star\beta$. Equation (23) can be rewritten in the form [cf. (21)]

$$x_\star\left[\frac{\xi + |1-x_\star|^2}{1-|x_\star|^2} + 1\right] = 1\ . \tag{24}$$

Since, according to (24), $x_\star$ must be a real number, one finally obtains

$$x_\star = 1 + \xi/2 \pm \sqrt{\xi^2/4+\xi}\,,\quad \mu_\star\beta = -\xi/2 \pm \sqrt{\xi^2/4+\xi}\ .$$

To guarantee stability of the closed-loop system one must require that $\mu_\star\beta > 0$ which leads to [cf. (5)] $\mu_\star\beta = \mu_o$. Since

$$\mu_\star = \arg\min_{\mu\in\mathrm{C}} R_{yy}(0;\mu) \tag{25}$$

the equilibrium point established above corresponds to the optimal (minimum-variance) control strategy.

B. Local stability

To prove stability of the equilibrium point we have to verify (15). Note that $R_{yz}(0;\mu) = -N(\mu)/D(\mu)$ where $N(\mu) = c_\mu[(1-\mu\beta)R_{yy}(0) - \sigma_v^2]$ and $D(\mu) = [1-(1-c_\mu)(1-\mu\beta)]\mu^*$. According to (23) it holds that $N(\mu_\star) = 0$. Additionally, since [cf. (25)] $R'_{yy}(0;\mu_\star) = 0$, one obtains $N'(\mu_\star) = -c_\mu\beta R_{yy}(0;\mu_\star)$. Combining these results one arrives at

$$\begin{aligned} f'(\mu_\star) = R'_{yz}(0;\mu_\star) = -\frac{N'(\mu_\star)}{D(\mu_\star)} \\ = \frac{c_\mu\mu_o R_{yy}(0;\mu_\star)}{|\mu_\star|^2[1-(1-c_\mu)(1-\mu_o)]} > 0 \end{aligned} \tag{26}$$

which proves that $\mu_\star$ is a stable equilibrium point.

C. Results for the normalized algorithm

Consider the normalized algorithm (10) where

$$\begin{aligned} \widehat{\mu}(t) = \widehat{\mu}(t-1) - \frac{y(t)z^*(t)}{r(t)} \\ r(t) = \rho r(t-1) + |z(t)|^2\ . \end{aligned} \tag{27}$$

Let $\gamma = 1-\rho$. For constant μ and for ρ sufficiently close to 1 it holds that $r(t) \cong h(\mu)/\gamma$ where $h(\mu) = \mathrm{E}[|z(t;\mu)|^2] = R_{zz}(0;\mu)$. Hence, the normalized algorithm can be analyzed analogously as the gradient algorithm (13) provided that the gain α is set to $\gamma R_{zz}^{-1}(0;\mu_\star)$. Note that this modification does not affect qualitative results reported in the previous subsections – similarly as before, $\mu_\star = \mu_o/\beta$ is the only stable equilibrium point of (27). The stochastic differential equation associated with (27) has the form

$$\begin{aligned} dX_s = -\gamma h^{-1}(\mu_\star)f'(\mu_\star)X_s ds \\ + \gamma h^{-1}(\mu_\star)\sqrt{g(\mu_\star)}\,dW_s\ . \end{aligned} \tag{28}$$

To evaluate $h(\mu_\star) = R_{zz}(0;\mu_\star)$ note that $\mathrm{E}[z(t)z^*(t)] = \mathrm{E}\{[(1-c_\mu)z(t-1) - c_\mu/\mu\, y(t-1)]\ [(1-c_\mu)z^*(t-1) - c_\mu/\mu^*\, y^*(t-1)]\}$, and hence

$$\begin{aligned} R_{zz}(0) = (1-c_\mu)^2 R_{zz}(0) - \frac{c_\mu(1-c_\mu)}{\mu^*}R_{zy}(0) \\ - \frac{c_\mu(1-c_\mu)}{\mu}R_{yz}(0) + \frac{c_\mu^2}{|\mu|^2}R_{yy}(0)\ . \end{aligned}$$

Since $R_{zy}(0;\mu_\star) = R_{yz}(0;\mu_\star) = 0$ one obtains

$$h(\mu_\star) = R_{zz}(0;\mu_\star) = R_{zz}^*(0;\mu_\star) = \frac{c_\mu R_{yy}(0;\mu_\star)}{|\mu_\star|^2(2-c_\mu)}\ . \tag{29}$$

D. Variability

To study stochastic variability of $\widehat{\mu}(t) - \mu_\star$ we have to evaluate $g(\mu_\star)$ in (16). To make computations easier we will assume that both noise sources are Gaussian

(**A4**) The noise sequences $\{v(t)\}$ and $\{w(t)\}$ are normally distributed.

Note that under (A1), (A2) and (A4) the processes $\{y(t)\}$ and $\{z(t)\}$ are also zero-mean and Gaussian. Therefore it holds that [11]

$$\begin{aligned}\eta(\tau;\mu_\star) &= \mathrm{E}[\, y(\tau;\mu_\star) z^*(\tau,\mu_\star) y^*(0;\mu_\star) z(0;\mu_\star)\,] \\ &= I_1(\tau) + I_2(\tau) + I_3(\tau)\end{aligned}$$

where

$$\begin{aligned}I_1(\tau) &= \mathrm{E}[\, y(\tau;\mu_\star) z^*(\tau,\mu_\star)\,]\, \mathrm{E}[\, y^*(0;\mu_\star) z(0;\mu_\star)\,] \\ &= |R_{yz}(0;\mu_\star)|^2\end{aligned}$$

$$\begin{aligned}I_2(\tau) &= \mathrm{E}[\, y(\tau;\mu_\star) y^*(0,\mu_\star)\,]\, \mathrm{E}[\, z^*(\tau;\mu_\star) z(0;\mu_\star)\,] \\ &= R_{yy}(\tau;\mu_\star) R^*_{zz}(\tau;\mu_\star)\end{aligned}$$

$$\begin{aligned}I_3(\tau) &= \mathrm{E}[\, y(\tau;\mu_\star) z(0,\mu_\star)\,]\, \mathrm{E}[\, z^*(\tau;\mu_\star) y^*(0;\mu_\star)\,] \\ &= R_{yz^*}(\tau;\mu_\star) R_{z^*y}(\tau;\mu_\star)\ .\end{aligned}$$

Since $R_{yz}(0;\mu_\star) = 0$, it holds that $I_1(\tau) \equiv 0$. Moreover, since the processes $\{v(t)\}$ and $\{w(t)\}$ were assumed to be circular white, one obtains $R_{vv^*}(\tau) = R_{ww^*}(\tau) = 0$, $\forall\tau$, which entails $R_{yz^*}(\tau;\mu_\star) = R_{z^*y}(\tau;\mu_\star) = 0$, $\forall\tau$ and leads to $I_3(\tau) \equiv 0$.
We will show that

$$R_{yy}(\tau;\mu_\star) = 0\ , \quad \forall\tau \neq 0\ . \tag{30}$$

Actually, note that

$$\begin{aligned}\mathrm{E}[y(t)y^*(t-1)] = \mathrm{E}\big\{ \big[&(1-\mu\beta)e^{j\omega_o} y(t-1) + w(t) \\ &+ v(t) - e^{j\omega_o} v(t-1) \big]\ y^*(t-1) \big\}\end{aligned}$$

which leads to $R_{yy}(1) = e^{j\omega_o}[(1-\mu\beta)R_{yy}(0) - R_{vy}(0)]$. In an analogous way one can show that $R_{yy}(\tau) = e^{j\omega_o}(1-\mu\beta)R_{yy}(\tau-1)$, $\forall\tau > 1$. Since [cf. (23)] $R_{yy}(1;\mu_\star) = e^{j\omega_o}[(1-\mu_\star\beta)R_{yy}(0;\mu_\star) - \sigma_v^2] = 0$, one obtains $R_{yy}(\tau;\mu_\star) = R^*_{yy}(-\tau;\mu_\star) = 0$, $\forall\tau \neq 0$, which is identical with (30).
Using (30) one arrives at

$$I_2(\tau) = \begin{cases} R_{yy}(0;\mu_\star) R_{zz}(0;\mu_\star) & \tau = 0 \\ 0 & \tau \neq 0 \end{cases}\ .$$

Finally, after combining all results presented above, one gets

$$g(\mu_\star) = \sum_{\tau=-\infty}^{\infty} \eta(\tau;\mu_\star) = R_{yy}(0;\mu_\star) R_{zz}(0;\mu_\star)\ . \tag{31}$$

Derivation of (31) in the non-Gaussian case, i.e. under (A1)–(A2) only, is also possible, but much more tedious.

III. TRACKING ANALYSIS

A. Algorithm (10)–(11)

Since the properties of the closed-loop system depend on the value of $\widehat{\mu}(t)\beta$, rather than on the value of $\widehat{\mu}(t)$, we will introduce a new variable $Y_s = \beta X_s$. Multiplying both sides of (28) with β one arrives at the following differential equation

$$\begin{aligned}dY_s = &-\gamma h^{-1}(\mu_\star) f'(\mu_\star) Y_s ds \\ &+ \gamma\beta h^{-1}(\mu_\star) \sqrt{g(\mu_\star)}\, dW_s\end{aligned} \tag{32}$$

which can be used to study the evolution of $\widehat{\mu}(t)\beta$ in the neighborhood of the equilibrium point $\mu_\star\beta = \mu_o$.
Using (26), (29) and (31) one can rewrite (32) in the form

$$dY_s = -bY_s ds + c\, dW_s \tag{33}$$

where

$$b = \gamma h^{-1}(\mu_\star) f'(\mu_\star) = \gamma\mu_o \frac{2 - c_\mu}{1 - (1-c_\mu)(1-\mu_o)} \tag{34}$$

$$c = \gamma\beta h^{-1}(\mu_\star)\sqrt{g(\mu_\star)} = \gamma|\mu_\star|\beta\sqrt{(2-c_\mu)/c_\mu}\ . \tag{35}$$

Note that neither b nor $|c| = \gamma\mu_o\sqrt{(2-c_\mu)/c_\mu}$ depend on β, which means that tracking properties of the modified RPE algorithm (12) are *independent* of the modeling error. Based on (33)–(35) one can rationalize the choice of γ and c_μ.

1) Selection of γ: Denote by $\mathrm{E}_\infty[|\widehat{\mu}(t)\beta - \mu_o|^2] \cong \mathrm{E}_\infty[|Y_s|^2]$ the variance of fluctuations of $\widehat{\mu}(t)\beta$ around μ_o. Solving the Lyapunov equation associated with (33) one obtains $\mathrm{E}_\infty[|Y_s|^2] = |c|^2/(2b)$, which leads to

$$\begin{aligned}q_\infty &= \mathrm{E}_\infty[|\widehat{\mu}(t)\beta - \mu_o|^2] \\ &\cong \gamma\mu_o \frac{1-(1-c_\mu)(1-\mu_o)}{2c_\mu}\ .\end{aligned} \tag{36}$$

Quite clearly, to make the steady-state fluctuations of $\widehat{\mu}(t)\beta$ small one should keep the coefficient γ sufficiently close to 0. On the other hand, as shown in [9], the closer that γ becomes to 0, the longer it takes for the algorithm to readjust the adaptation gain $\widehat{\mu}(t)$ when the plant changes. Hence selection of γ is a classical variance/bias compromise, typical of identification of nonstationary systems [12]: for “small” values of γ the estimation algorithm is “slow” (yields large tracking bias) but “accurate” (yields small tracking variance), whereas for “large” values of γ it is “fast” but “inaccurate”.

2) Selection of c_μ: According to [9], the constant c_μ should be chosen so as to minimize the following measure of the tracking capability of the algorithm:

$$J(c_\mu) = \frac{b^2}{|c|^2} = \frac{(2-c_\mu)c_\mu}{[1-(1-c_\mu)(1-\mu_o)]^2}\ .$$

Straightforward calculations lead to

$$c_\mu^o = \arg\min_{c_\mu} J(c_\mu) = \mu_o\ . \tag{37}$$

Note that in the case where $\sqrt{\xi} \ll 1$ (slow rate of amplitude variation) it holds that $\mu_o \cong \sqrt{\xi} = \sigma_w/\sigma_v$ [cf. (5)]. Then, for $c_\mu = \mu_o$, one obtains: $b = \gamma$, $|c| \cong \gamma\sqrt{2\mu_o}$ and $q_\infty \cong \gamma\mu_o$.

B. Algorithm (9)–(10)

Careful examination of all results derived in Section II leads to the conclusion that the differential equation associated with the original RPE algorithm (9)–(11) is identical with (33), provided that the coefficient c_μ, appearing in (34)–(35), is replaced with $\mu_\star = \mu_o/|\beta|$. Note that after such substitution the coefficients b and $|c|$ depend on β. This means that

c_μ	0.005	0.01	0.05	0.1
$K_1(q^{-1})$	0.010	0.010	0.010	0.010
$K_2(q^{-1})$	0.010	0.010	0.011	0.011
$K_3(q^{-1})$	0.011	0.011	0.013	0.016

TABLE I
STEADY-STATE MEAN VALUES OF $\widehat{\mu}(t)\beta$ FOR THREE PLANTS AND DIFFERENT CHOICES OF c_μ

tracking characteristics of (9), such as the rate of adaptation or steady-state accuracy, depend not only on the user-defined tuning parameters (γ) but also on modeling errors (β), which are unknown. From the practical viewpoint this is certainly an undesirable feature of the original RPE algorithm, making it less attractive than the modified algorithm (11).

IV. SIMULATION RESULTS

A. Equilibrium point

Table I shows the mean steady-state values of $|\widehat{\mu}(t)\beta|$ for three first-order plants and different choices of c_μ. The plants were described by the following transfer functions: $K_1(q^{-1}) = 1$ (inertionless), $K_2(q^{-1}) = 0.5/(1-0.5q^{-1})$ (small inertia) and

$$K_3(q^{-1}) = \frac{0.0952}{1-0.9048q^{-1}} \tag{38}$$

(large inertia). The last model was adopted from the paper of Guo and Bodson [4], and corresponds to a continuous-time plant with transfer function $G(s) = 1/(1+0.01s)$, sampled at the rate of 1 kHz. In all cases the same modeling error was introduced: $|\beta| = 1.5$, $\mathrm{Arg}\beta = 60^o$. The algorithm (10)–(11) was used with $\rho = 0.999$. The disturbance and noise settings were equal to $\sigma_v = 0.1$, $\sigma_w = 0.001$, $\omega_0 = 0.1$ and $d(0) = 1$. Under such conditions the optimal value of μ is equal to $\mu_o \cong 0.01$. The values shown in Table I were obtained by combined ensemble averaging (50 realizations of $\{v(t)\}$ and $\{w(t)\}$) and time averaging (100000 time-steps). For each realization, the first 25000 samples were discarded to ensure that only the steady-state values are averaged.
Table I shows that for inertial plants the steady-state values of $\widehat{\mu}(t)\beta$ differ from μ_o. Since all theoretical results were derived using the inertionless system approximation (6), this discrepancy is not a surprise . The amount of bias depends on the inertia of the controlled plant and can be decreased by lowering the value of c_μ. It is marginal for the optimal choice of c_μ ($c_\mu = \mu_o = 0.01$) but may be substantial when the adopted value of c_μ is too large.

B. Variability

Dependence of the steady-state variance of $\widehat{\mu}(t)\beta$ on $\gamma = 1-\rho$ was measured – in an analogous way as described in the previous subsection and under the same disturbance and noise conditions – for the Guo & Bodson's plant $K_3(q^{-1})$. Figure 1 shows results obtained for $\beta = 1$ (no modeling error) and for $\beta = 4$. Similarly as in the previous experiment, the constant c_μ was set to 0.01. Note good correspondence

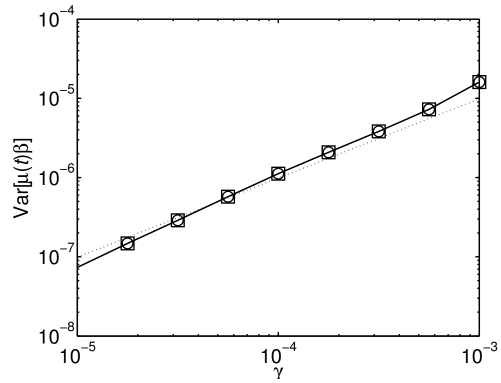

Fig. 1. Dependence of the steady-state variance of $\widehat{\mu}(t)\beta$ on γ for the Guo & Bodson's plant $K_3(q^{-1})$. Solid lines - experimental results, dotted lines - theoretical predictions. Circles - $\beta = 1$, squares - $\beta = 4$.

between experimental and theoretical curves in the considered range of RPE gains. The obtained results are practically insensitive to inertia of the controlled plant and to modeling errors.
For $\gamma > 0.003$ the bursting type of behavior can be occasionally observed. Hence, in this range of γ, averaging does not yield representative results. The intensity of bursts grows with γ. Bursts arise in a classical scenario. Too large values of $\widehat{\mu}(t)$ cause temporal instability of the system. However, since rapid growth of the output signal speeds up convergence of $\widehat{\mu}(t)$ to μ_o/β, the closed-loop stability is quickly regained. Since bursts are practically inacceptable, some sort of safety jacketing is needed – see [7] for more details.
The discrepancy between experiment and theory, observed for "large" values of γ, can be easily explained. First, the stochastic differential equation, which led to (36), is an asymptotic description of the closed-loop system, valid only for sufficiently small values of γ. Second, since γ is the "adaptation rate of the adaptation rate μ", it should take much smaller values than $\widehat{\mu}(t)$. Such recommendation is consistent with the rule saying that adaptation time constants of a hierarchical multi-layer adaptive system should gradually increase from the bottom (the lowest adaptation level) to the top (the highest adaptation level). Note that in the case considered the inequality $\gamma \ll \mu_o$ is satisfied when $\gamma \leq 0.001$ (assuming that the term "much smaller" is interpreted as "at least 10 times smaller").

C. Transient performance

The objective of this simulation experiment was to demonstrate the ability of the proposed algorithm to cope with sudden plant changes. The Guo & Bodson's plant $K_3(q^{-1})$ was switched at the instant $t = 15000$ to the plant described by $K_4(q^{-1}) = 0.3/(1-0.8q^{-1})$. The noise and disturbance settings were the same as in the previous examples. Fig. 2 shows the averaged results of 100 simulation runs, obtained for the algorithm (10)–(11) equipped with $c_\mu = 0.01$ and $\rho = 0.999$. The nominal plant gain was fixed at $k_n = 1$. The corresponding modeling errors were equal to: $|\beta| = 0.707$,

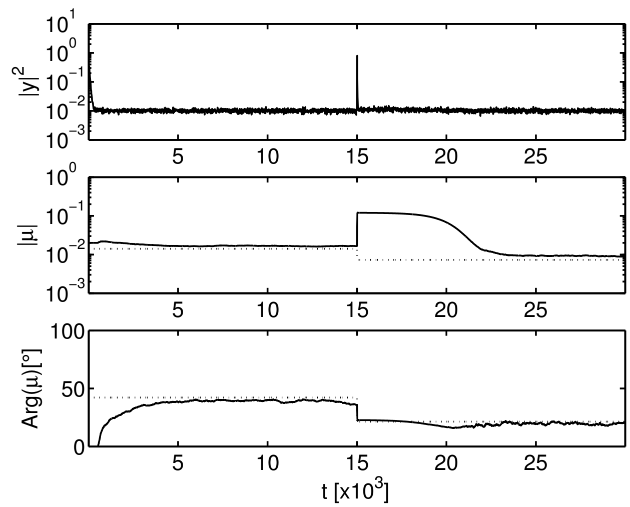

Fig. 2. Mean transient behavior of the disturbance rejection algorithm (average results of 100 simulation runs). Solid lines – ensemble averages of the estimated values, dotted lines – optimal steady-state values.

$\mathrm{Arg}\beta = -42.2^\circ$ for $t < 15000$ and $|\beta| = 1.34$, $\mathrm{Arg}\beta = -21.4^\circ$ for $t \geq 15000$.

During the first 500 time-steps the quantities $z(t)$, $r(t)$ and $\widehat{\mu}(t)$ were not evaluated – they were kept at their starting values $z(0) = 0$, $r(0) = 100$, $\widehat{\mu}(0) = 0.02$ and not updated. Then, at the instant $t = 501$, the adaptation lock was released.

According to Fig. 2 the algorithm converges in the mean to settings that are close to the optimal steady-state settings. It deals favorably with an abrupt plant change. Just after the change, the magnitude of the adaptation gain $\widehat{\mu}(t)$ temporarily increases to quickly compensate large initial modeling errors; later on it gradually decays to settle down around its optimal steady-state value. Note very quick response to phase errors and (usually) much slower response to magnitude errors – the effect caused by diverse sensitivity of system output to two types of modeling errors.

The mean transient response is shorter than 50 samples, i.e. it lasts for less than one period of the disturbance ($T_o = 2\pi/\omega_o \cong 63$).

D. Tracking under nonstandard conditions

To enable theoretical analysis we have assumed that the amplitude of the sinusoidal disturbance evolves according to the random-walk model. The aim of our last numerical example was to demonstrate that the proposed gain-tuning mechanism works correctly also under "nonstandard" conditions. The Guo & Bodson's plant $K_3(q^{-1})$ was subject to a sinusoidal disturbance with a sinusoidally varying amplitude

$$a(t) = 1 + 0.15 \sin(2\pi t/10000) \ .$$

Although the theoretical value of the optimal adaptation gain is not known in this case, one has the right to expect that μ_o should be time-varying – it should take smaller values when $a(t)$ varies slowly (i.e. when the absolute value of the derivative $a'(t)$ is small), and larger when $a(t)$ varies faster. This is confirmed by the results summarized in Table II, where the algorithm (10)–(11), with adaptively tuned μ, is confronted with the algorithm (7) equipped with a constant gain. Since the algorithm (7) cannot compensate modeling errors, to make the comparison fair the true plant gain was assumed to be known ($\beta = 1$). Note that the adaptive algorithm yields better performance than any variant of the constant-gain algorithm. This clearly demonstrates robustness of the proposed solution.

μ	0.01	0.02	0.03	0.04
$\mathrm{E}[\|y(t)\|^2]$	0.01059	0.01022	0.01020	0.01022

μ	0.05	0.06	0.07	Adaptive
$\mathrm{E}[\|y(t)\|^2]$	0.01026	0.01031	0.01036	0.01018

TABLE II

STEADY-STATE PERFORMANCE OF A CONSTANT-GAIN DISTURBANCE REJECTION ALGORITHM (FOR SEVERAL VALUES OF μ) AND OF ITS ADAPTIVE VERSION.

V. CONCLUSION

Tracking properties of an (earlier proposed) adaptive vibration controller can be studied by examining the stochastic differential equation associated with the closed-loop system. Using this technique we have shown that the analyzed control scheme converges locally in the mean to the optimal regulator. Additionally, we have formulated several useful "rule of thumb" design guides allowing one to increase robustness and statistical efficiency of vibration control.

REFERENCES

[1] Fuller, C.R., S.J. Elliott and P.A. Nelson (1995). *Active control of vibration*. Academic Press, New York.
[2] Kuo, S.M. and D.R. Morgan (1996). *Active Noise Control Systems: Algorithms and DSP Implementations*. Wiley-IEEE Press, New York.
[3] Wu, B. and M. Bodson (2004). Multi-channel active noise control for periodic sources – indirect approach. *Automatica*, vol. 40, 203–212.
[4] Guo, X. and M. Bodson (2007). Adaptive rejection of multiple sinusoids of unknown frequency. *Proc. European Control Conference*, Kos, Greece, 121–128.
[5] Landau I.D., A. Constantinescu & D. Rey (2005). Adaptive narrow band disturbance rejection applied to an active suspension – an internal model principle approach. *Automatica*, vol. 41, 563–574.
[6] Landau I.D. & D.I. Patrascu (2007). Rejection of unknown multiple narrow band disturbances – a direct adaptive control approach. *Proc. European Control Conference*, Kos, Greece, 135–141.
[7] Niedźwiecki, M. and M. Meller (2008). A study in vibration control: the unknown plant – known frequency case. Gdańsk University of Technology, Technical Report # ETI-1/2008, http://www.eti.pg.gda.pl/katedry/ksa/pracownicy/Maciej.Niedzwiecki.
[8] Niedźwiecki, M. and M. Meller (2008). New approach to adaptive vibration control. *Proc. 47th CDC*, Cancun, Mexico.
[9] Benveniste, A. and G. Ruget (1982). A measure of the tracking capability of recursive stochastic algorithms with constant gains. *IEEE Trans. Automat. Contr.*, vol. 25, 788–794.
[10] Benveniste, A., M. Métivier and P. Priouret (1990). *Adaptive Algorithms and Stochastic Approximations*. Springer-Verlag.
[11] Haykin, S. (1996). *Adaptive Filter Theory*. Prentice Hall, Englewood Cliffs NJ.
[12] Niedźwiecki, M. (2000). *Identification of Time-varying Processes*. Wiley. New York.